Journal of Cellular Biochemistry 104:2310–2323 (2008)

Sparc Localizes to the Blebs of Hobit Cells and Human Primary Osteoblasts

Giovanna Baldini,[1] Cristina Ponti,[1]* Roberta Bortul,[1] Paola Narducci,[1] Vittorio Grill,[1] and Alberto M. Martelli[2]

[1]Department of Biomedicine, Section of Morphology, University of Trieste, via Manzoni 16, 34138 Trieste, Italy
[2]Department of Human Anatomical Sciences, Cell Signalling Laboratory, University of Bologna, via Irnerio 48, 40126 Bologna, Italy

Abstract Secreted protein acidic and rich in cystein (SPARC) is a secreted glycoprotein involved in several biological processes such as tissue remodeling, embryonic development, cell/extracellular matrix interactions, and cell migration. In particular, SPARC affects bone remodeling through the regulation of both differentiation/survival of osteoblasts and bone extracellular matrix synthesis/turnover. Here, we investigated SPARC subcellular localization in the human osteoblastic HOBIT cell line by immunocytochemistry and western blot analysis. We show that, under normal exponential cell growth conditions, SPARC localized both to cell nucleus and to cytoplasm, with no co-localization on actin stress fibers. However, in colchicine-treated HOBIT cells and human primary osteoblasts undergoing blebs formation, SPARC showed a different cellular distribution, with an additional marked compartmentalization inside the blebs, where it co-localized with globular actin and actin-binding proteins such as α-actinin, cortactin, and vinculin. Moreover, we demonstrate by an in vitro assay that the addition of SPARC to actin and α-actinin inhibited the formation of cross-linked actin filaments and disrupted newly formed filaments, most likely due to a direct interaction between SPARC and α-actinin, as indicated by immunoprecipitation assay. The specific silencing of SPARC RNA expression markedly decreased the ability of colchicine-treated HOBIT cells to undergo blebbing, suggesting a direct role for SPARC in cell morphology dynamics during cytoskeletal reorganization. J. Cell. Biochem. 104: 2310–2323, 2008.

Key words: SPARC; F-actin; cell blebs; α-actinin; HOBIT

The matricellular proteins are extracellular proteins which do not contribute structurally to the extracellular milieu as the classical extracellular matrix proteins, but modulate interactions between extracellular matrix and cells. SPARC is a calcium-binding glycoprotein belonging to matricellular proteins. SPARC is composed of three structural domains with distinct modular functions [Hohenester et al., 1996, 1997]. SPARC is highly expressed during embryogenesis, while its presence becomes more restricted in adult tissues and cells, which include bone, activated human platelets, and megakaryocytes [Brekken and Sage, 2001]. Moreover, SPARC is consistently detected under conditions of cellular stress, such as endotoxin stimulation, heat shock, wound repair, and tissue remodeling [Bradshaw and Sage, 2001; Bradshaw et al., 2002] as well as in tumorigenesis. Indeed, SPARC expression is increased in cell lines and in invasive malignant cells from breast, prostate, lung, and skin cancers even though SPARC role in cell transformation has not been yet elucidated [Porter et al., 1995; Ledda et al., 1997; Lecrone et al., 2000; Thomas et al., 2000; Briggs et al., 2002; Koukourakis et al., 2003; Jones et al., 2004].

In addition, several reports demonstrated that SPARC regulates some important biological

Giovanna Baldini and Cristina Ponti contributed equally to this work.

Grant sponsor: Italian Ministry of Innovation, University and Scientific Research M.I.U.R-FIRB 2001; Grant number: RBAU01EX8K; Grant sponsor: CARISBO Foundation; Grant sponsor: Contract Grant Sponsor: University of Bologna, Progetti Strategici EF2006.

*Correspondence to: Cristina Ponti, PhD, Department of Biomedicine, Section of Morphology, University of Trieste, via Manzoni 16, 34138 Trieste, Italy. E-mail: cponti@units.it

Received 2 August 2007; Accepted 21 March 2008

DOI 10.1002/jcb.21789

processes, including cell cycle progression and cell adhesion to the extracellular proteins, by altering cell shape [Bradshaw et al., 1999]. The anti-proliferative effects have been correlated to SPARC action during the terminal differentiation due, at least partially, to signal transduction modulation via a G-protein coupled receptor. In fact, SPARC is overexpressed during the terminal differentiation of keratinocytes and the disruption of SPARC locus in the mice resulted in the abnormal differentiation of lens fibers [Norose et al., 1998; Bradshaw et al., 2002; Yan et al., 2002]. SPARC can lead to a cytoskeletal rearrangement essential for cell transmigration, by binding to VCAM-1, a surface molecule mediating leukocyte adhesion [Kelly et al., 2007], and can also alter cell shape by an important counter-adhesive function achieved by dissolution of focal adhesion complexes and reorganization of actin stress fibers [Murphy-Ullrich et al., 1995]. This inhibition of cell adhesion gives rise to modifications in cell shape that are correlated with the induction of apoptosis, even though these changes may be temporarily necessary for cells undergoing migration and proliferation. In particular, the addition of recombinant SPARC to cultured cells causes either focal adhesion disassembly, or prevention of cell spreading and inhibition of proliferation [Funk and Sage, 1991; Murphy-Ullrich et al., 1995; Motamed and Sage, 1998; Hudson et al., 2005].

An interesting mechanism of cell cytoskeleton reorganization is represented by cell blebbing. Cell blebs appear like local herniations of the plasma membrane [Harris, 1990] and can be associated with apoptosis and drug treatment [Laster and Mackenzie, 1996], but also with physiological processes such as mitosis [Laster and Mackenzie, 1996] and development [Trinkaus, 1973]. Interestingly, cell blebbing is a well-known example of dramatic reorganization of cytoskeleton during cell migration [Keller and Bebie, 1996; Yoshida and Inouye, 2001], involving a first phase of bleb expansion, with detachment of plasma membrane from cell actin cortex, followed by a second phase of F-actin polymerization on bleb rim with consequent retraction [Cunningham, 1995; Keller and Eggli, 1998]. The layer of detached actin cortex, remaining at the "neck" of the bleb, acts like a sieve, impeding the entry of cell nucleus, RER, Golgi apparatus, and other organelles inside the blebs [Keller and Eggli, 1998].

It is also noteworthy that SPARC plays an important role in the skeletal tissues embryogenesis and in the bone homeostasis and fracture healing. Hence, SPARC is constantly detected in the pericellular matrix surrounding osteoblasts and osteocytes and is also involved in the process of endochondral ossification modulating the new bone formation [Delany et al., 2005]. Studies on knockout mice demonstrated that when SPARC gene was disrupted, a progressive age-associated osteopenia was observed, related to a decreased number of osteoblasts and osteoclasts [Bornstein and Sage, 2002]. Moreover, the mesenchymal cells isolated from SPARC-null mice displayed an increased likelihood to differentiate into adipocytes rather than osteoblasts [Framson and Sage, 2004]. In addition, studies carried out in SPARC-deficient mice treated by recombinant SPARC, have demonstrated that SPARC selectively supports the migration towards bone of highly metastatic cells [De et al., 2003] suggesting a possible involvement of SPARC in the regulation of these lesions.

Although SPARC has been extensively studied in the bone, particularly with regards to SPARC interactions with the extracellular matrix, the role and the localization of intracellular SPARC and its relationship with cytoskeletal remodeling and cell migration of osteoblasts have not been investigated yet. Here, we analyzed the intracellular localization of SPARC in a human osteoblastic cell model, HOBIT cells, which closely resemble the mature osteoblasts phenotype, and studied both the intracellular localization of SPARC during blebbing of colchicine-treated HOBIT cells and primary osteoblasts, and its interaction with actin and specific actin-binding proteins.

MATERIALS AND METHODS

Cell Culture

HL60, Jurkat, and MCF-7 cells were grown in RPMI 1640 medium, supplemented with 10% fetal calf serum (FCS), 2 mM L-glutamine, 100 U/ml penicillin, 100 μg/ml streptomycin (all purchased from Sigma–Aldrich, St. Louis, MO). Simian virus-40-immortalized hOB cells (HOBIT) were kindly provided by Prof. B Lawrence Riggs, Mayo Foundation (Rochester, MN). Cells were grown in Dulbecco's minimal essential medium (DMEM, Sigma–Aldrich) supplemented with 10% FCS, 2 mM

L-glutamine, antibiotics and 1% non-essential amino acids (Gibco, Grand Island, NY). Human primary osteoblasts (Promocell, Heidelberg, Germany) were grown in DMEM/F-12 (Sigma–Aldrich) supplemented with 10% FCS, 2 mM L-glutamine, antibiotics, and 10^{-3} M pyruvic acid.

Indirect Immunofluorescence

HOBIT cells, primary osteoblasts, and MCF-7 cells were grown on glass coverslips for 48 h and fixed for 20 min at room temperature (RT) with 4% paraformaldehyde in PBS. Jurkat and HL60 cells were cytospinned onto glass slides, then immediately fixed as above. To induce cell blebbing in HOBIT cells and primary osteoblasts, colchicine was added to a final concentration of 10^{-4} M for 30 min at 37°C. Cells were then fixed as above, permeabilized with 0.3% Triton X-100 in PBS for 10 min at RT, washed with PBS and then blocked with 4% bovine serum albumin (BSA), 5% normal goat serum in PBS.

Double immunofluorescence labeling for SPARC and α-actinin was performed using the following primary antibodies: anti-SPARC IgG mouse monoclonal antibody (mAb) (AON-5031; Haematologic Technologies, Essex Junction, VT) and anti-α-actinin IgM mAb (Sigma–Aldrich). Briefly, coverslips were first incubated with anti-SPARC mAb (1:50) followed by incubation with Cy3-conjugate anti-mouse IgG (1:400; Jackson ImmunoResearch Laboratories Inc., West Grove, PA). After washing, slides were incubated with anti-α-actinin mAb (1:100) and then incubated with FITC-conjugate anti-mouse IgM (μ-chain specific, 1:100; Sigma–Aldrich). Negative controls were performed either by means of an irrelevant mAb or by omitting the primary antibody. To label F-actin, FITC-phalloidin was employed (1:50 of 6.6 μM stock solution, for 30 min at RT, as recommended by the manufacturer, Molecular Probes, Invitrogen Detection Technologies, Carlsbad, CA).

To label G-actin, AlexaFluor 594-conjugate deoxyribonuclease I (DNase I) was employed (1:1,000 for 30 min at RT; Molecular Probes, Invitrogen Detection Technologies).

Double labeling for F-actin and SPARC or cortactin, or vinculin, or fibronectin was performed by firstly incubating samples with the primary antibody followed by the appropriate secondary antibody, and then incubating with FITC-phalloidin.

Primary antibodies used were: (i) anti-human vinculin IgG_1 mAb (clone hVIN-1; 1:200, Sigma–Aldrich); (ii) anti-cortactin IgG_1 mAb (p80/85, clone F11; 1:100, Upstate Biotechnology, Lake Placid, NY); (iii) anti-fibronectin rabbit IgG (1:100, Sigma–Aldrich). The secondary antibodies used were anti-mouse IgG Cy3-conjugate (1:400) for vinculin and cortactin, and anti-rabbit IgG Cy3-conjugate (1:100, Sigma–Aldrich) for fibronectin, respectively.

Double labeling for SPARC and G-actin was performed by first labeling with anti-SPARC mAb and anti-mouse IgG FITC-conjugate (1:100, Sigma–Aldrich) and then incubating with AlexaFluor 594-conjugate DNase I.

Images were collected with a CoolSnap video-camera (Roper Scientific Inc., Tucson, AZ) connected to a Zeiss Axiophot microscope (Carl Zeiss, Germany).

Preparation of Whole Cell Extracts and Isolated Nuclei

Cells (HL60, Jurkat, MCF-7, HOBIT) were cultured in 10 cm dishes for 48 h under exponential growth conditions, as SPARC levels decrease after this stage of growth. Cells were collected by centrifugation, washed with PBS and sonicated with Sonoplus (Bandelin Electronic, GmbH & Co., KG, Germany) for 20 s. Samples were then dissolved in 4× sample buffer (0.25 M Tris–Cl pH 6.8, 8% SDS, 40% glycerol, 20% 2-mercaptoethanol) for SDS gel electrophoresis.

To determine SPARC protein nuclear localization, isolation of nuclei was performed by hypotonic shock, as previously described [Martelli et al., 1991]. Briefly, cells were washed once in PBS and then resuspended in 10 mM Tris–HCl, pH 7.4, 2 mM $MgCl_2$, 0.5 mM phenylmethylsulfonyl fluoride (PMSF), 1 μg/ml each of aprotinin and leupeptin (TM-2 buffer, at a temperature of 10°C). After 5 min at 0°C, Triton X-100 was added to 0.5% (w/v) and cells were sheared by one passage through a 22 gauge needle fitted to a 30 ml plastic syringe. Nuclei were sedimented at 400*g* for 6 min, resuspended in TM-5 buffer (TM-2 buffer with 5 mM $MgCl_2$) and centrifuged at 400*g* for 8 min. Isolated nuclear fractions were resuspended in lysis buffer containing 25 mM Tris–HCl, pH 7.4, 1 mM EDTA, 1 mM EGTA, 1 mM PMSF, and Complete Protease Inhibitor cocktail (Roche

Diagnostics GmbH, Mannheim, Germany). Samples were then dissolved in 4× electrophoresis sample buffer and incubated at 95°C for 5 min.

Western Blot Analysis

Whole cell extracts and isolated nuclei were resolved electrophoretically on 10% SDS–polyacrylamide gels and proteins were transferred to nitrocellulose membranes. Membranes were incubated with a 1:1,000 dilution of anti-SPARC mAb. To detect tubulin, membranes were incubated with a 1:2,000 dilution of anti-β-tubulin mAb, while, to detect SC-35, an anti-splicing factor SC-35 mAb was used (from Sigma–Aldrich). Blots were further incubated with a 1:2,000 dilution of peroxidase-conjugate anti-mouse IgG antibody (from Sigma–Aldrich). Protein bands on the membrane were detected by the Lumi-Light Plus Western Blotting Substrate (Roche Diagnostics).

Electron Microscopy

To induce cell blebbing, HOBIT cells were grown on glass coverslips for 48 h, then treated with colchicine as above. After a brief rinse in PBS, samples were fixed with 2.5% glutaraldehyde in 0.1 M phosphate buffer, pH 7.3, for 10 min at RT, and then for 20 min at 4°C. Samples were then rinsed in 0.1 M phosphate buffer, pH 7.3, postfixed with 1% osmium tetroxide (Electron Microscopy Sciences, Washington, PA) in the same buffer for 1 h at 4°C, dehydrated in alcohol, and then treated with propylene oxide. After embedding in Durcupan ACM (Electron Microscopy Sciences), ultrathin sections of cell monolayers were cut with a Reichert OM ultramicrotome (Reichert-Jung, Wien, Austria). Sections were stained with uranyl acetate and lead citrate, and then examined with a Jeol 100S electron microscope (Jeol, Japan) operated at 80 kV.

Actin Polymerization In Vitro Assay

Actin polymerization in vitro assay was performed as follows: purified rabbit soleus muscle actin (16 μM, Sigma–Aldrich) stored in Ca-ATP buffer (2 mM imidazole, 0.1 mM $CaCl_2$, 0.5 mM DTT, 0.2 mM ATP) was polymerized by the addition of 1/10 volume of exchange buffer (10 mM EDTA, 1 mM $MgCl_2$) for 10 min at RT, followed by the addition of 1/10 volume of 1 M KCl for 1 h at RT. The actin mixtures were then diluted 1:4 with Mg-ATP buffer (2 mM imidazole, 0.1 mM $MgCl_2$, 0.5 mM DTT, 0.2 mM ATP) in the presence of purified chicken gizzard α-actinin (250 nM, Sigma–Aldrich) [Coghill et al., 2003]. Samples were kept overnight at RT, then added with FITC-phalloidin to a final concentration of 1 μM. A drop of each suspension was mounted on a microscope slide and images were collected with a CoolSnap video-camera connected to a Zeiss Axiophot microscope at 60× magnification.

To study SPARC effect on actin polymerization, 30 μg/ml [Bradshaw et al., 1999] bovine bone SPARC (Calbiochem, Darmstadt, Germany) was added to 100 μl of actin suspension prior to beginning the assay or at the end, before FITC-phalloidin addition.

Immunoprecipitation

Antibody conjugated beads were prepared by mixing 30 μl of protein G-Sepharose 4 Fast Flow (1:2 in PBS; GE Healthcare Bio-Sciences AB, Uppsala, Sweden) and either 1 μg of anti-SPARC mAb or 1 μg of an irrelevant mAb as a control in 0.5 ml ice-cold PBS, followed by incubation for 2 h in a tube rotator at 4°C. HOBIT cells grown in 100 mm dishes were scraped in 1 ml of non-denaturing lysis buffer [1% (w/v) Triton X-100, 50 mM Tris–Cl, pH7.4, 300 mM NaCl, 5 mM EDTA, 0.02 (w/v) sodium azide, protease inhibitors] and incubated for 30 min. Lysates were cleared by microcentrifugation at 16,000*g* for 15 min and the supernatants were then collected, added with 10 μl of 10% BSA in PBS, and kept under agitation for 1 h at 4°C with the G-Sepharose-conjugated antibodies. After several washes (0.1% Triton X-100, 50 mM Tris–Cl, pH 7.4, 300 mM NaCl, 5 mM EDTA), the complexes of G-Sepharose and bound proteins were resuspended in electophoresis sample buffer, boiled for 5 min and resolved onto an 8% SDS–polyacrylamide gel. Western blot was performed as described above, by incubating membranes with a 1:1,000 dilution of anti-α-actinin IgM mAb.

RNA Interference (siRNA)

HOBIT cells were seeded as described above and 24 h later (when confluence was about 50%) were washed with serum-free DMEM, and then transfected in the same medium. For SPARC silencing, we have used the siGenome Smart pool (M-003710-02-0005) for human SPARC or

the siControl Non-Targeting siRNA as a negative control (both purchased from Dharmacon Inc., Chicago, IL). siRNAs were diluted with siRNA buffer (Dharmacon) to a final concentration of 20 pmol/μl and transfection performed using Lipofectamine™ 2000 (Invitrogen). Twenty-four hours after plating, HOBIT cells transfected with siGenome Smart for SPARC or with non-targeting RNA, were re-plated onto Petri dishes and 72 h after transfection, cells were tested for SPARC expression by western blot analysis and in parallel treated with colchicine, as described above.

RESULTS

SPARC Is Detected in Nuclear and Cytoplasmic Cell Compartments of HOBIT Cells

SPARC subcellular distribution is still debated, as some recent reports highlighted a nuclear staining for SPARC in human urothelial [Hudson et al., 2005] and immortalized murine lens epithelial cells [Yan et al., 2005], even though other studies demonstrated only a cytoplasmic localization. In several cell lines, intracellular SPARC has been co-localized to endoplasmic reticulum and Golgi complex, presumably destined for secretion [Lane and Sage, 1994], while Gooden et al. [1999] presented evidence that the distribution of endogenous, intracellular SPARC can vary according to specific phases of the cell cycle. Hence, we analyzed intracellular SPARC protein distribution by different approaches in HOBIT cells and in other cell lines, to examine whether the detection of nuclear SPARC could be related to a specific cell type.

In a first set of experiments SPARC subcellular distribution has been evaluated by indirect immunofluorescence staining both in suspension- (HL60, Jurkat) and adherent-growing (MCF-7, HOBIT) cell lines under exponential growth conditions (Fig. 1A). Immunofluorescence analysis for SPARC in HL60 cells evidenced no staining, suggesting a lack of SPARC expression in this cell line. Interestingly, both Jurkat and MCF-7 cells displayed a fluorescent signal for SPARC in the cytoplasm, while nuclear staining was detectable in MCF-7 but not in Jurkat cells. HOBIT cells showed both cytoplasmic and nuclear localization. The intensity of cytoplasmic staining for SPARC detected in HOBIT cells was lower than that displayed by MCF-7 cells, but it is noteworthy that HOBIT cells showed a stronger positivity for nuclear SPARC than MCF-7 cells. Replacement of anti-SPARC mAb with an irrelevant mAb or omission of the primary antibody resulted in no staining in all cell lines evaluated (not shown). We then performed western blot analysis on whole cell extracts (Fig. 1B) and isolated nuclei (Fig. 1C) to confirm the results obtained by immunocytochemistry. As expected, HOBIT and MCF-7 cells were positive for SPARC both in nuclear fraction and whole cell extracts. In contrast, SPARC was detected only in whole cell extracts in Jurkat cells, while HL60 cells did not express SPARC protein in any cellular compartments. Since the purity of isolated nuclei is critical, contamination of nuclei by cytoplasmic proteins was monitored by tubulin protein analysis. As expected, we detected only a faint band corresponding to tubulin in all nuclear samples, while a strong immunoreactive band was detectable in whole cell extracts. SC-35 nuclear protein was also analyzed to show equal loading of nuclear fraction for all the samples.

SPARC Localizes to Cell Blebs of HOBIT and Human Primary Osteoblasts

Cell blebs are structures where actin cortex is reorganized and cortex-free membrane is transiently generated. Cell blebbing is often associated to unfavorable cell conditions, such as apoptosis, but also to physiological processes, like cell migration [Keller and Bebie, 1996; Yoshida and Inouye, 2001]. Hence, we evaluated the formation and retraction of cell blebs in living HOBIT cells (Fig. 2). HOBIT cells were grown on glass coverslips for 48 h and then treated with 10^{-4} M colchicine, an agent able to disrupt microtubules by binding to tubulin and preventing its polymerization. After 30 min treatment, HOBIT cells exhibited the formation of transient cell blebs, that retracted in about 60 s (Fig. 2, Panels A,B), as documented by optical microscopic analysis. This phenomenon is not specific for HOBIT cells, as it has also been described in other cell types [Keller and Zimmermann, 1986; Keller and Eggli, 1998]. In a parallel analysis, we observed cell bleb morphology also by transmission electron microscopy (TEM) (Fig. 2, Panel C). TEM analysis demonstrated that cell blebs appeared like evident protrusions of plasma membrane, associated with a thin actin layer at the bleb rim. At the "neck" of the bleb, it was noticed a thick F-actin layer, connected with cell actin

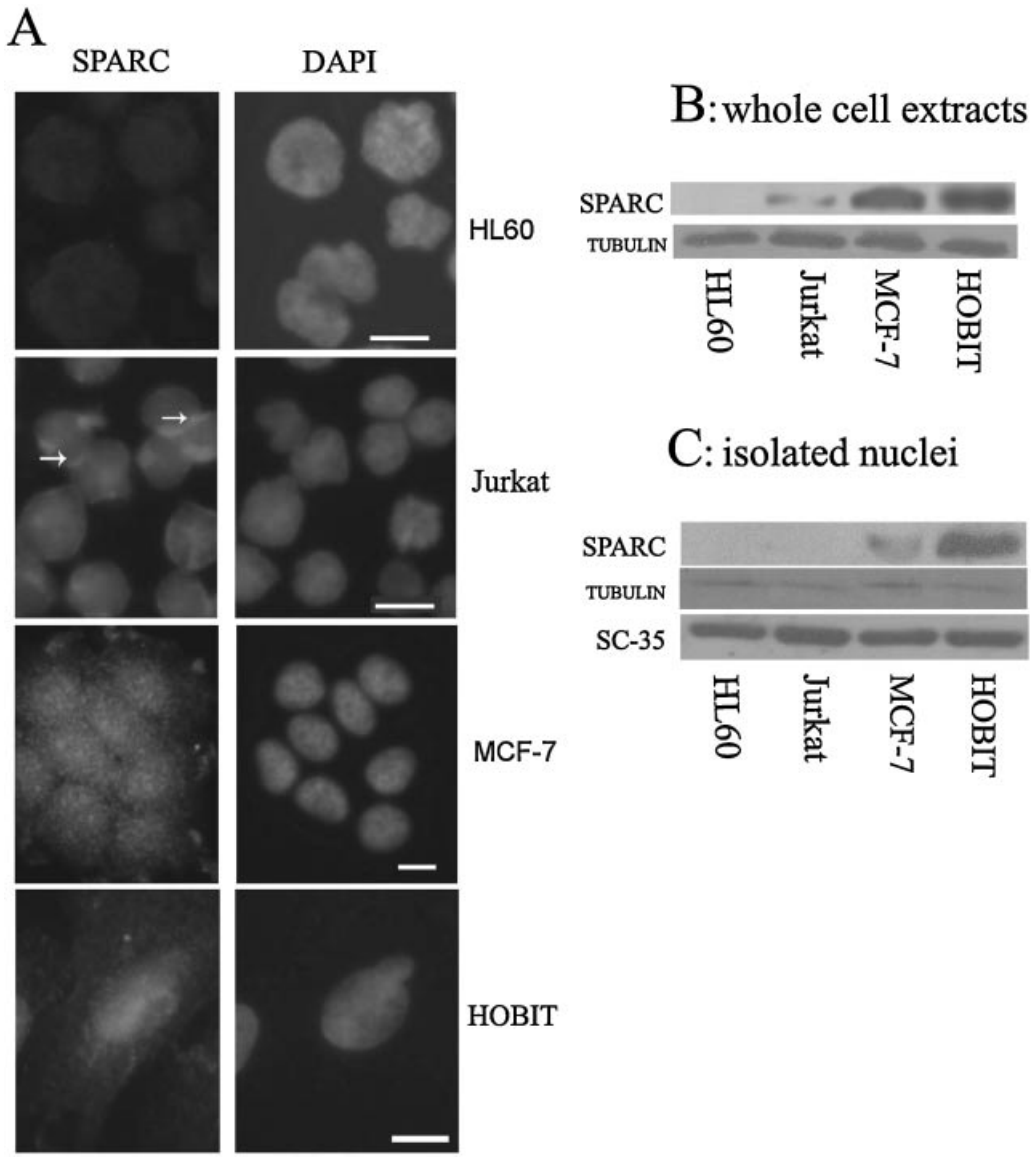

Fig. 1. SPARC expression in HL60, Jurkat, MCF-7, and HOBIT cells. **Panel A**: SPARC immunofluorescence analysis. In HL60 cells, SPARC was not expressed (negative control). In Jurkat cells, SPARC was expressed only in cytoplasm, with accumulation at the sites of contact among cells (see arrows). In MCF-7 and HOBIT cells, SPARC was expressed both in cell nucleus and cytoplasm. DAPI staining visualized nuclei. Calibration bar: 10 μm. **Panels B**,**C**: Western blot analysis for SPARC expression in whole cell extracts (Panel B) and isolated nuclei (Panel C) of HL60, Jurkat, MCF-7, and HOBIT cells. Tubulin was detected to demonstrate equal loading of whole cell extracts and to rule out major cytoplasmic contamination of isolated nuclei. Immunodetection of SC-35 nuclear protein demonstrated equal loading of nuclear fractions. HL60 cells did not express SPARC (negative control). Jurkat cells expressed SPARC in whole cell extracts, but were SPARC negative in the nuclear fraction. MCF-7 cells expressed SPARC in whole cell extract, with a weaker band in the nuclear fraction. HOBIT cells displayed SPARC expression both in whole cell extract and in the nuclear fraction.

cortex. As expected [Keller and Eggli, 1998], mitochondria or other organelles were not detectable inside the blebs.

Since cell blebs are currently considered as a cellular modification necessary for migration and shape remodeling, and SPARC is involved in cell migration and in the reorganization of bone tissue and extracellular matrix, we further analyzed by immunofluorescence staining the presence of SPARC in cell blebs. As a cellular model, we used both HOBIT cells and human primary osteoblasts, in order to rule out that HOBIT cell cytoskeleton might have undergone some alterations related to cell passage, as

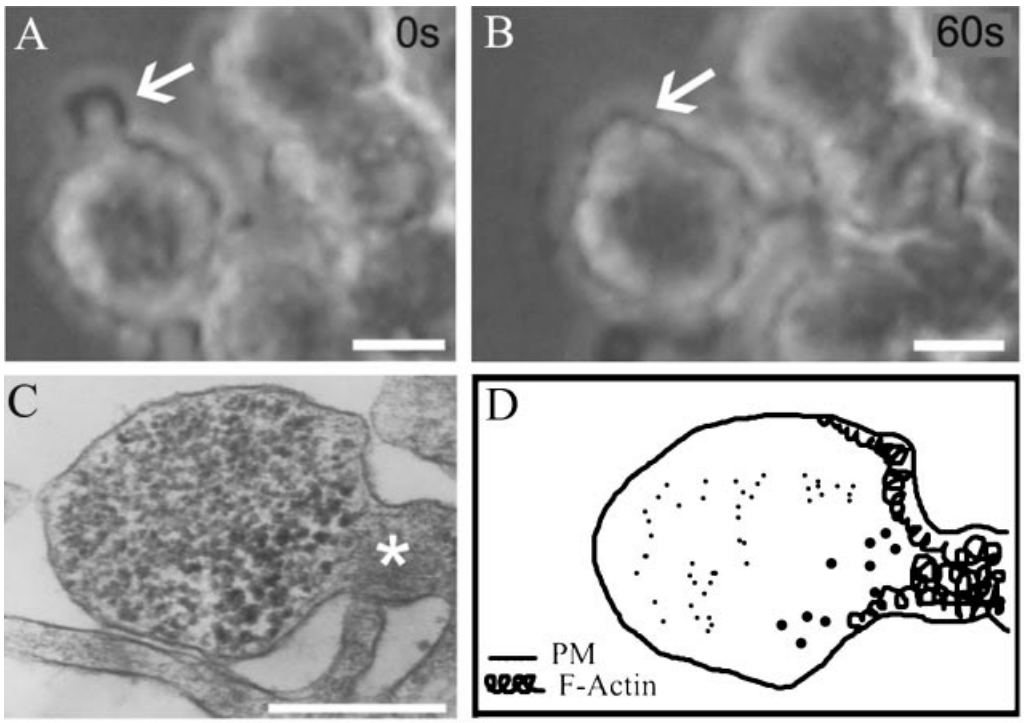

Fig. 2. Microscopical and ultrastructural analysis of cell bleb formation. HOBIT cells were grown on coverslips for 48 h and then treated with 10^{-4} M colchicine at 37°C for 30 min. **Panel A**: Phase contrast light microscopy of a cell bleb of a colchicine-treated living HOBIT cell. **Panel B**: The same cell observed 60 s later. Cell bleb appeared to retract on cell surface, nearly disappearing. Calibration bar A,B: 10 μm. **Panel C**: TEM analysis of a colchicine-treated HOBIT cell bleb. Cell blebs appear like protrusions of cell membrane filled with granules. The rim of the bleb beneath the plasma membrane is partially covered by an F-actin cortex, while F-actin filaments are not present in the bleb core. At the ''neck'' of the bleb, it could be noticed a thick F-actin layer that was not associated with the plasma membrane (see asterisk). Calibration bar: 1 μm. **Panel D**: Graphic representation of bleb structure shown in Panel C.

previously described by others [Segarini et al., 1989; Galustian et al., 1995].

At first, we carried out SPARC detection in untreated HOBIT cells and human primary osteoblasts, to determine if SPARC co-localizes with phalloidin-stained stress fibers. This staining is a reliable method to understand whether a given cell component co-localizes with F-actin, which composes the actin cortex and is also present in actin stress fibers. Interestingly, SPARC did not co-localize with phalloidin-stained stress fibers (Figs. 3A and 4A) suggesting that SPARC does not interact with steady state F-actin fibers.

In HOBIT cells treated with colchicine, SPARC distribution was different if compared with untreated cultures. In fact, in untreated cells, SPARC was detectable in the nucleus and cytoplasm and did not co-localize with phalloidin-stained stress fibers (Fig. 3A). In contrast, after treatment with colchicine, following an at least partial stress fiber disassembly, the formation of several blebs, clearly delimited by an F-actin ring (Fig. 3B), was consistently observed, and, remarkably, SPARC localized inside the blebs, despite the maintenance of a diffuse cytoplasmic and nuclear staining. In a parallel analysis performed on primary human osteoblasts, a similar pattern of SPARC distribution was detected in both untreated and colchicine-treated cells (Fig. 4A,B).

We next investigated whether SPARC may share cell bleb localization with three actin-binding proteins, represented by α-actinin (a protein cross-linking actin filaments), vinculin (a focal adhesion protein) and cortactin (a podosome protein). As shown in Figures 3 and 4, α-actinin, vinculin, and cortactin co-localized with SPARC inside cell blebs, in colchicine-treated HOBIT cells and human primary osteoblasts cells. The localization of these proteins involved in cytoskeleton rearrangement was specific, because fibronectin,

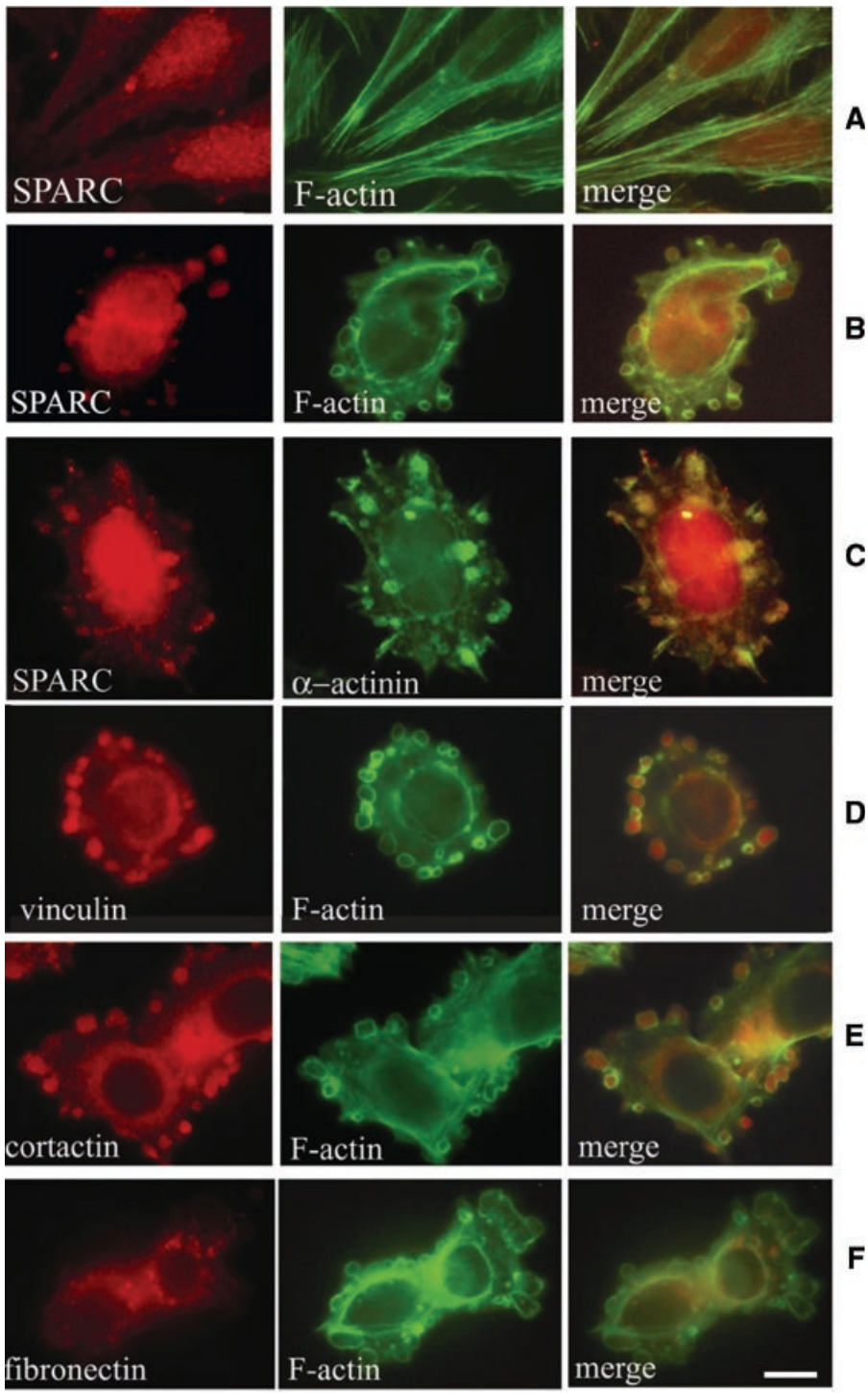

Fig. 3. Immunofluorescence analysis for SPARC, α-actinin, vinculin, cortactin, and fibronectin in HOBIT cells. **Panels A**,**B**: Immunolocalization of SPARC and phalloidin-stained F-actin in strongly adherent and colchicine-treated HOBIT cells, respectively. **Panel C**: Immunolocalization of SPARC and α-actinin in colchicine-treated HOBIT cells. **Panel D**: Immunolocalization of vinculin and F-actin in colchicine-treated HOBIT cells. **Panel E**: Immunolocalization of cortactin and phalloidin-stained F-actin in colchicine-treated HOBIT cells. **Panel F**: Immunolocalization of fibronectin and phalloidin-stained F-actin in colchicine-treated HOBIT cells. Calibration bar: 10 μm. For all the panels, the merged images are shown at right.

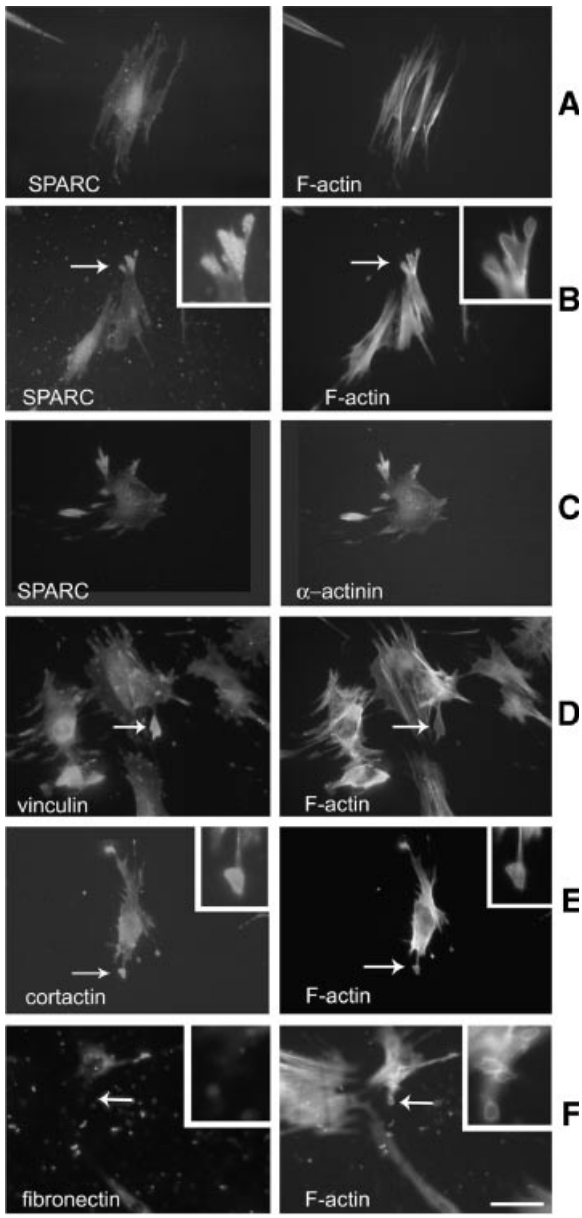

Fig. 4. Immunofluorescence analysis for SPARC, α-actinin, vinculin, cortactin and fibronectin in human primary osteoblasts. **Panels A,B**: Immunolocalization of SPARC and phalloidin-stained F-actin in strongly adherent and colchicine-treated human primary osteoblasts, respectively. As indicated by the arrow, SPARC compartmentalization inside blebs was as in HOBIT cells (insert 2× magnification). **Panel C**: Immunolocalization of SPARC and α-actinin in colchicine-treated osteoblasts. **Panel D**: Immunolocalization of vinculin and F-actin in colchicine-treated osteoblasts. **Panel E**: Immunolocalization of cortactin and phalloidin-stained F-actin in colchicine-treated osteoblasts (insert 2× magnification). **Panel F**: Immunolocalization of fibronectin and phalloidin-stained F-actin in colchicine-treated osteoblasts (insert 2× magnification). Arrows indicate the position of representative cell blebs. Calibration bar: 50 μm.

an adhesion glycoprotein of the extracellular matrix, did not localize inside the blebs (Fig. 4F).

SPARC Co-Localizes With G Actin in Blebs and Prevents Actin/α-Actinin Polymerization In Vitro

It is noteworthy that SPARC localized to almost all of cell blebs (~99%), even if staining intensity for SPARC was different. This observation is clearly evidenced in a large field picture of the experiments described above, which showed that in colchicine-treated HOBIT cells SPARC localized inside all the blebs (Fig. 5A,B). Moreover, by means of fluorescent DNase I, which selectively labels G actin, we were able to demonstrate that blebs contain G-actin which co-localized with SPARC (Fig. 5C,D).

Bleb formation is a consequence of microtubule disassembly and modifications of cross-linking state of cellular actin. To determine whether SPARC may influence actin polymerization, we used an in vitro assay with purified cytoskeleton components. It is well known that addition of α-actinin to actin suspension in vitro leads to the formation of cross-linked α-actinin/actin filaments that can be clearly evidenced by immunofluorescence staining [Coghill et al., 2003]. Therefore, in a first set of in vitro experiments, we observed that addition of α-actinin to actin suspension induced the formation of cross-linked actin filaments, whereas adding SPARC after induction of cross-linked actin filaments led to the complete disruption of these structures (Fig. 5E). It is noteworthy that when SPARC was added at the same time as actin and α-actinin, the cross-linked filaments did not form (Fig. 5E).

To confirm these observations, we performed an immunoprecipitation analysis using HOBIT whole cell lysates incubated with two different immunocomplexes consisting of either an irrelevant antibody or an anti-SPARC mAb. This technique demonstrated the existence of in vivo interactions between α-actinin and SPARC (Fig. 5F).

Taken together, our findings indicated, for the first time to our knowledge, a direct role for SPARC to inhibit cross-linked actin filament assembly in the presence of α-actinin by means of an interaction with α-actinin.

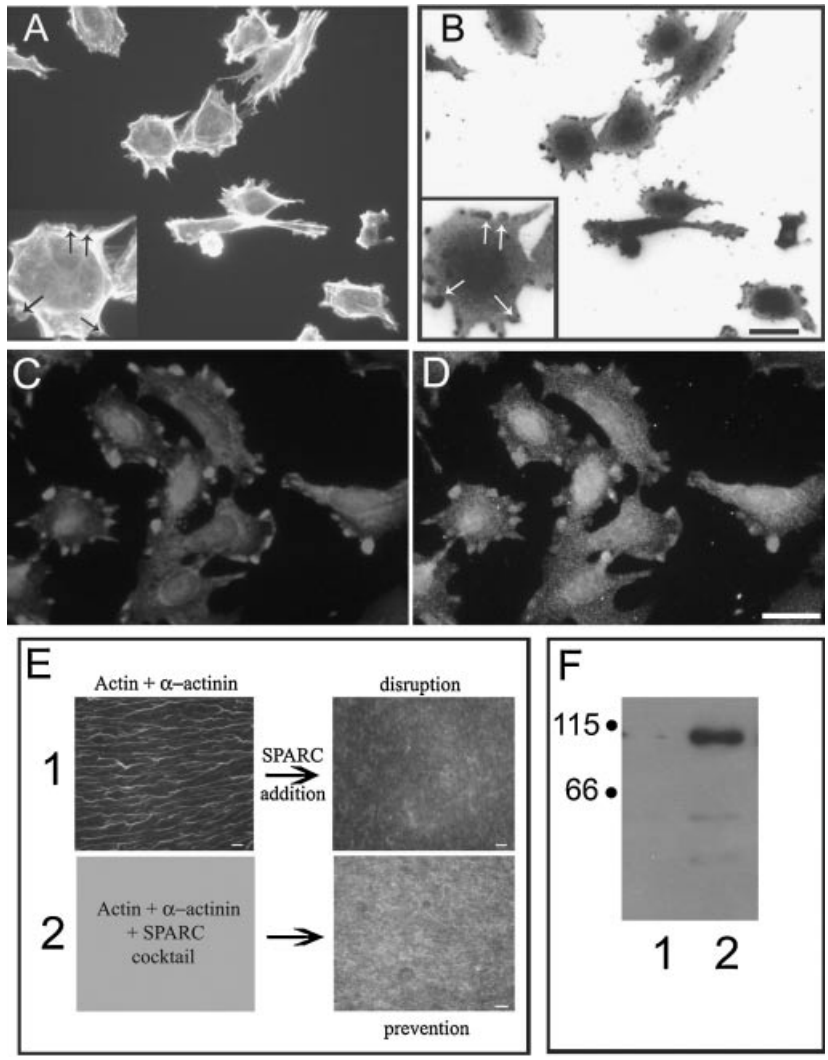

Fig. 5. SPARC and G-actin co-localize in cell blebs, and SPARC prevents in vitro α-actinin-dependent actin polymerization. **Panel A**: Phalloidin-stained F-actin in several colchicine-treated HOBIT cells. Arrows indicate four cells blebs in a representative cell (insert magnification 2×). **Panel B**: Immunolocalization of SPARC in the same field as in Panel 1. Image has been converted into a white background picture and its contrast enhanced to better visualize SPARC localization. Arrows highlight the presence of intense SPARC labeling in the blebs corresponding to Panel 1 insert. SPARC appears to localize in the vast majority of cell blebs (about 99%), even if with different staining intensities. **Panel C**: G-actin labeling with Alexa Fluor 594-conjugate DNase I in colchicine treated HOBIT cells. **Panel D**: SPARC immunolocalization in the same field as in Panel C. Calibration bars 10 μm. **Panel E**: (1) The addition of α-actinin to actin suspension in vitro determined the formation of cross-linked actin filaments, here clearly visualized by immunofluorescence staining. The addition of bovine bone SPARC to the solution led to the disruption of these filaments; (2) The addition of SPARC at the same time as actin and α-actinin prevented the formation of cross-linked actin filaments. Calibration bars: 10 μm. **Panel F**: Detection of α-actinin after immunoprecipitation of HOBIT whole cells lysates with different immunocomplexes obtained with an irrelevant antibody (**lane 1**) or anti-SPARC mAb (**lane 2**). Molecular mass markers are denoted in kDa on the left.

SPARC Silencing Prevents Cell Blebbing in HOBIT Cells

The knockdown of SPARC has been previously associated with a decreased ability of cells to detach from substrate following trypsinization [Bradshaw et al., 1999] and to undergo contraction [Barker et al., 2005]. Thus, we studied the effect of SPARC silencing on cell bleb formation in HOBIT cells. HOBIT cells transfected with non-targeting siRNA or siGenome Smart for SPARC, respectively, were treated with colchicine, and then analyzed for the localization of phalloidin-stained F-actin. While cells transfected with non-targeting siRNA maintained the ability to form cell blebs

(Fig. 6A), HOBIT cells with a silenced SPARC prevalently displayed an altered flat morphology, with still evident F-actin formations and a strong decrease in the number of cell blebs (Fig. 6B). The effective silencing of SPARC by specific siRNA was demonstrated by western blot analysis (Fig. 6C).

DISCUSSION

The analysis of normal distribution of intracellular SPARC in HOBIT cells demonstrated a diffuse localization of this protein in both the nucleus and the cytoplasm. SPARC detection in the nucleus was specific, in fact two different technical approaches confirmed this observation and parallel analysis of different cell lines demonstrated cell type specific patterns of SPARC distribution. Although SPARC cytoplasmic localization has been described by several authors, nuclear localization is controversial. SPARC is a secreted protein easily detected in the cytoplasm of several cell lines and primary cells in a Golgi-associated perinuclear location [Lane and Sage, 1994]. A previous report [Gooden et al., 1999] has highlighted that SPARC localized to the nucleus during specific cell cycle phases. Moreover, Yan et al. [2005] described a translocation of SPARC to the nucleus of lens epithelial cells and SPARC nuclear localization has also been observed in urothelial cells [Hudson et al., 2005]. In addition, it has been very recently demonstrated that recombinant SPARC can be internalized in the cell and be translocated to cell nucleus where it inhibits DNA synthesis [Kosman et al., 2007].

It is known that SPARC can interact with integrin-linked-kinase on cell membrane, promoting the formation of fibronectin-induced stress fibers [Barker et al., 2005]. In light of these findings, we decided to study the possible role of SPARC in mediating important aspects of cell migration/motility by directly regulating cytoskeletal organization.

We treated HOBIT cells and, in parallel, human primary osteoblasts with colchicine, in order to determine possible changes in the intracellular distribution of SPARC, with a main focus on cell blebs. Cell blebs are

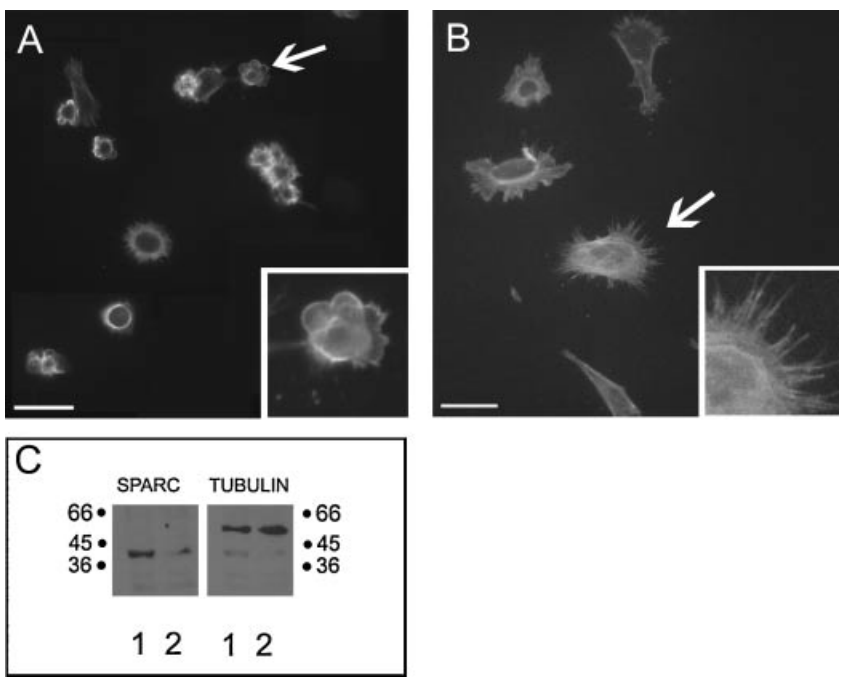

Fig. 6. Effect of SPARC silencing on cell bleb formation in HOBIT cells. **Panels A**,**B**: Immunolocalization of phalloidin-stained F-actin in colchicine-treated HOBIT cells transfected with non-targeting siRNA or siGenome Smart for SPARC, respectively. As indicated by the arrow in Panel A, colchicine-treated HOBIT cells transfected with non-targeting siRNA still formed cell blebs. In contrast, as indicated by the arrow in Panel B, colchicine-treated HOBIT cells transfected with siGenome Smart for SPARC, displayed the prevalence of an altered flat morphology, with still evident F-actin formations and a strong decrease in the number of detectable cell blebs. Calibration bar: 10 μm. **Panel C**: Western blot analysis for SPARC and tubulin expression in HOBIT cells transfected with non-targeting siRNA (**lane 1**) or siGenome Smart for SPARC (**lane 2**).

protrusions characterized by a typical spherical shape and sudden formation, appearing like local herniations of the plasma membrane [Harris, 1990]. Blebs have been observed in several cell types, and can be associated with unfavorable conditions, such as apoptosis and drug treatment [Laster and Mackenzie, 1996], or with physiological processes such as mitosis [Laster and Mackenzie, 1996] and development [Trinkaus, 1973]. Cell blebbing represents also a well-known example of dramatic reorganization of the cytoskeleton during cell migration [Keller and Bebie, 1996; Yoshida and Inouye, 2001]. Cell blebs are dynamic structures that can transform into lamellipodia and vice versa [Trinkaus, 1973; Keller et al., 1984] during ameboid movement of adherent cells. [Webb and Horwitz, 2003]. Bleb formation is a consequence of microtubule disassembly and modifications of cross-linking state of cellular actin. A recent study on the reassembly of contractile actin cortex in cell blebs [Charras et al., 2006] has demonstrated the existence of a temporal sequence of protein recruitment to the cell membrane during cell bleb formation. Bleb formation is composed of two distinct phases: first, an expansion phase, where plasma membrane detaches from the actin cortical cytoskeleton, which instead remains intact at the cell base and then, as a result of the myosin II-driven contraction of the actin cortex and the generation of intracellular pressure transients, bleb is inflated. Later on, a bleb retraction phase takes place, characterized by a progressive recruitment of actin on bleb membrane, leading to a new F-actin cortex at the bleb rim and consequent bleb retraction [Cunningham, 1995; Keller and Eggli, 1998]. In particular, bleb retraction appears to be related to a new actin polymerization along its cytoplasmic surface [Cunningham, 1995], driven by a sequential recruitment of a large array of proteins at the bleb membrane [Charras et al., 2006]. In this context, the cortical actin remaining at the site of membrane detachment during bleb expansion, the so-called "restriction ring" [Keller and Eggli, 1998], is thought to act like a sieve, blocking the entry of cellular organelles and nucleus inside the bleb, but still allowing the permeation of solutes and, only in some cases, small vesicles, not tethered to cytoskeletal elements [Hagmann et al., 1999]. Scanning electron microscopy analysis of bleb actin revealed a structure composed of an interconnected network of actin filaments [Charras et al., 2006]. However, despite of all these intriguing observations, the complete mechanism of actin reorganization at the membrane of newly generated blebs still remains unclear. Our data showed that SPARC dramatically changed its distribution in HOBIT cells treated with colchicine. SPARC clearly localized to the great majority of the blebs, however SPARC staining intensity in the blebs was variable, possibly due to blebbing phase (expansion or retraction). Remarkably, when we compared SPARC distribution with α-actinin distribution, they appeared to co-localize to the blebs of HOBIT cells and primary osteoblasts. Vinculin and cortactin also showed compartmentalization in the bleb, while fibronectin, a protein with secretory features similar to SPARC, did not. Therefore, our observations, and especially SPARC different staining intensity inside the blebs of a same cell, support the model of the cell bleb as a dynamic organized structure, where actin polymerization follows discrete intervals regulated by a temporal sequence of actin binding and contractile protein recruitment [Charras et al., 2006].

The bleb represents a cytoplasmic-based compartment inside the cell, independent but at the same time connected to the cytoplasm and to intracellular signaling by an actin interconnected network. The presence of endogenous SPARC compartmentalization inside the bleb may suggest SPARC as a new key regulatory element in actin reorganization at the bleb, both during plasma membrane detachment from the cortex and actin reorganization/polymerization at the restriction ring or at the rim of the bleb. Interestingly, by labeling HOBIT cells with fluorescent DNase I, we were able to demonstrate that SPARC co-localizes with G actin within the blebs.

Moreover, our set of in vitro experiments demonstrated that SPARC, when added to a soluble actin/α-actinin suspension, directly affected the formation of α-actinin cross-linked actin filaments, and also led to the disruption of new filaments. This is, at least to our knowledge, the first demonstration of a direct effect of SPARC on actin filament formation in vitro. These findings were also supported by a parallel immunoprecipitation assay which demonstrated the existence of an in vivo interaction between SPARC and α-actinin in HOBIT cells.

Silencing of SPARC expression in HOBIT cells, followed by treatment with colchicine, prevented the induction of blebbing. F-actin formations were still detected but cells exhibited a prevalence of an altered flat morphology, at least in the time interval analyzed (short term).

This phenomenon is supported by a previous observation by Bradshaw et al. [1999], who demonstrated that SPARC-null mesenchimal cells are generally more spread when compared with their wild-type counterpart, and present an increased resistance to trypsinization, a treatment leading to cell detachment and bleb formation. Moreover, it has also been demonstrated that lack of SPARC in fibroblasts induced the inhibition of cell contraction via a reduced capability to assemble fibronectin into fibrils [Barker et al., 2005].

Therefore, if the effect of SPARC we observed in vitro is also present in vivo, SPARC could be regarded as a new key candidate for actin cytoskeleton reorganization via α-actinin cross-linkage regulation. Our study opens new perspectives in the investigation of SPARC functions, interactions and signaling events.

Altogether our data yield new insight into the possible SPARC function in osteoblasts where this protein is able to interact with actin, the master regulator of cytoskeleton structure, cell shape modulation, and cell migration. These biological effects also suggest that SPARC may play a pivotal role in bone homeostasis and fracture repair.

REFERENCES

Barker TH, Baneyx G, Cardo-Vila M, Workman GA, Weaver M, Menon PM, Dedhar S, Rempel SA, Arap W, Pasqualini R, Vogel V, Sage EH. 2005. SPARC regulates extracellular matrix organization through its modulation of integrin-linked kinase activity. J Biol Chem 280: 36483–36493.

Bornstein P, Sage EH. 2002. Matricellular proteins: Extracellular modulators of cell function. Curr Opin Cell Biol 14:608–616.

Bradshaw AD, Sage EH. 2001. SPARC, a matricellular protein that functions in cellular differentiation and tissue response to injury. J Clin Invest 107:1049–1054.

Bradshaw AD, Francki A, Motamed K, Howe C, Sage EH. 1999. Primary mesenchymal cells isolated from SPARC-null mice exhibit altered morphology and rates of proliferation. Mol Biol Cell 10:1569–1579.

Bradshaw AD, Reed MJ, Sage EH. 2002. SPARC-null mice exhibited accelerated cutaneous wound healing. J Histochem Cytochem 50:1–10.

Brekken RA, Sage EH. 2001. SPARC, a matricellular protein: At the crossroads of cell-matrix communication. Matrix Biol 19:816–827.

Briggs J, Chamboredon S, Castellazzi M, Kerry JA, Bos TJ. 2002. Transcriptional upregulation of SPARC, in response to c-Jun overexpression, contributes to increased motility and invasion of MCF7 breast cancer cells. Oncogene 21:7077–7091.

Charras GT, Hu CK, Coughlin M, Mitchison TJ. 2006. Reassembly of contractile actin cortex in cell blebs. J Cell Biol 175:477–490.

Coghill ID, Brown S, Cottle DL, McGrath MJ, Robinson PA, Nandurkar HH, Dyson JM, Mitchell CA. 2003. FHL3 is an actin-binding protein that regulates α-actinin-mediated actin bundling: FHL3 localizes to actin stress fibers and enhances cell spreading and stress fiber disassembly. J Biol Chem 278:24139–24152.

Cunningham CC. 1995. Actin polymerization and intracellular solvent flow in cell surface blebbing. J Cell Biol 129:1589–1599.

De S, Chen J, Narizhneva NV, Heston W, Brainard J, Sage EH, Byzova TV. 2003. Molecular pathway for cancer metastasis to bone. J Biol Chem 278:39044–39050.

Delany AM, Kalajzic I, Bradshaw AD, Sage EH, Canalis E. 2005. Osteonectin-null mutation compromises osteoblast formation, maturation and survival. Endocrinology 144: 2588–2596.

Framson PE, Sage EH. 2004. SPARC and tumor growth: Where the seed meets the soil? J Cell Biochem 92:679–690.

Funk SE, Sage EH. 1991. The Ca^{2+}-binding glycoprotein SPARC modulates cell cycle progression in bovine aortic endothelial cells. Proc Natl Acad Sci USA 88:2648–2652.

Galustian C, Dye J, Leach L, Clark P, Firth JA. 1995. Actin cytoskeletal isoforms in human endothelial cells in vitro: Alteration with cell passage. In Vitro Cell Dev Biol Anim 31:796–802.

Gooden MD, Vernon RB, Bassuk JA, Sage EH. 1999. Cell cycle-dependent nuclear location of the matricellular protein SPARC: Association with the nuclear matrix. J Cell Biochem 74:152–167.

Hagmann J, Burger MM, Dagan D. 1999. Regulation of plasma membrane blebbing by the cytoskeleton. J Cell Biochem 73:488–499.

Harris AK. 1990. Protrusive activity of the cell surface and the movements of tissue cells. In: Akkas N, editor. Biomechanics of active movement and deformation of cells. Berlin: Springer-Verlag. pp 249–294.

Hohenester E, Maurer P, Hohenadl C, Timpl R, Jansonius JN, Engel J. 1996. Structure of a novel extracellular Ca(2+)-binding module in BM-40. Nat Struct Biol 3: 67–73.

Hohenester E, Maurer P, Timpl R. 1997. Crystal structure of a pair of follistatin-like and EF-hand calcium-binding domains in BM-40. EMBO J 16:3778–3786.

Hudson AE, Feng WC, Delostrinos CF, Carmean N, Bassuk JA. 2005. Spreading of embryologically distinct urothelial cells is inhibited by SPARC. J Cell Physiol 202:453–463.

Jones C, Mackay A, Grigoriadis A, Cossu A, Reis-Filho JS, Fulford L, Dexter T, Davies S, Bulmer K, Ford E, Parry S, Budroni M, Palmieri G, Neville AM, O'Hare MJ, Lakhani SR. 2004. Expression profiling of purified normal human

luminal and myoepithelial breast cells: Identification of novel prognostic markers for breast cancer. Cancer Res 64:3037–3045.

Keller HU, Bebie H. 1996. Protrusive activity quantitatively determines the rate and direction of cell locomotion. Cell Motil Cytoskeleton 33:241–251.

Keller H, Eggli P. 1998. Protrusive activity, cytoplasmic compartmentalization, and restriction rings in locomoting blebbing Walker carcinosarcoma cells are related to detachment of cortical actin from the plasma membrane. Cell Motil Cytoskeleton 41:181–193.

Keller HU, Zimmermann A. 1986. Shape changes and chemokinesis of Walker 256 carcinosarcoma cells in response to colchicine, vinblastine, nocodazole and taxol. Invasion Metastasis 6:33–43.

Keller HU, Naef A, Zimmermann A. 1984. Effects of colchicine, vinblastine and nocodazole on polarity, motility, chemotaxis and cAMP levels of human polymorphonuclear leukocytes. Exp Cell Res 153:173–185.

Kelly KA, Allport JR, Yu AM, Sinh S, Sage EH, Gerszten RE, Weissleder R. 2007. SPARC is a VCAM-1 counterligand that mediates leukocyte transmigration. J Leuk Biol 81:748–756.

Kosman J, Carmean N, Leaf EM, Dyamenahalli K, Bassuk JA. 2007. The motif of SPARC that inhibits DNA synthesis is not a nuclear localization signal. J Mol Biol 24:883–901.

Koukourakis MI, Giatromanolaki A, Brekken RA, Sivridis E, Gatter KC, Harris AL, Sage EH. 2003. Enhanced expression of SPARC/osteonectin in the tumor-associated stroma of non-small cell lung cancer is correlated with markers of hypoxia/acidity and with poor prognosis of patients. Cancer Res 63:5376–5380.

Lane TF, Sage EH. 1994. The biology of SPARC, a protein that modulates cell-matrix interactions. FASEB J 8:163–173.

Laster SM, Mackenzie JM. 1996. Bleb formation and F-actin distribution during mitosis and tumor necrosis factor-induced apoptosis. Microsc Res Tech 34:272–280.

Lecrone V, Li W, Devoll RE, Logothetis C, Farach-Carson MC. 2000. Calcium signals in prostate cancer cells: Specific activation by bone-matrix proteins. Cell Calcium 27:35–42.

Ledda F, Bravo AI, Adris S, Bover L, Mordoh J, Podhajcer OL. 1997. The expression of the secreted protein acidic and rich in cysteine (SPARC) is associated with the neoplastic progression of human melanoma. J Invest Dermatol 108:210–214.

Martelli AM, Falcieri E, Gobbi P, Manzoli L, Gilmour RS, Cocco L. 1991. Heat-induced stabilization of the nuclear matrix: A morphological and biochemical analysis in murine erythroleukemia cells. Exp Cell Res 196:216–225.

Motamed K, Sage EH. 1998. SPARC inhibits endothelial cell adhesion but not proliferation through a tyrosine phosphorylation-dependent pathway. J Cell Biochem 70: 543–552.

Murphy-Ullrich JE, Lane TF, Pallero MA, Sage EH. 1995. SPARC mediates focal adhesion disassembly in endothelial cells through a follistatin-like region and the Ca(2+)-binding EF-hand. J Cell Biochem 57:341–350.

Norose K, Lo WK, Clark JI, Sage EH, Howe C. 1998. SPARC deficiency leads to early onset cataractogenesis. Invest Ophtalmol Vis Sci 39:2674–2680.

Porter PL, Sage EH, Lane TF, Funk SE, Gown AM. 1995. Distribution of SPARC in normal and neoplastic human tissue. J Histochem Cytochem 43:791–800.

Segarini PR, Rosen DM, Seyedin SM. 1989. Binding of transforming growth factor-beta to cell surface proteins varies with cell type. Mol Endocrinol 3:261–272.

Thomas R, True LD, Bassuk JA, Lange PH, Vessella RL. 2000. Differential expression of osteonectin/SPARC during human prostate cancer progression. Clin Cancer Res 6:1140–1149.

Trinkaus JP. 1973. Surface activity and locomotion of Fundulus deep cells during blastula and gastrula stages. Dev Biol 30:69–103.

Webb DJ, Horwitz AF. 2003. New dimensions in cell migration. Nat Cell Biol 5:690–692.

Yan Q, Clark JI, Wight T, Sage EH. 2002. Alterations in the lens capsule contributes to cataractogenesis in SPARC-null mice. J Cell Sci 115:2747–2756.

Yan Q, Weaver M, Perdue N, Sage EH. 2005. Matricellular protein SPARC is translocated to the nuclei of immortalized murine lens epithelial cells. J Cell Physiol 203: 286–294.

Yoshida K, Inouye K. 2001. Myosin II-dependent cylindrical protrusions induced by quinine in Dictyostelium: Antagonizing effects of actin polymerization at the leading edge. J Cell Sci 114:2155–2165.